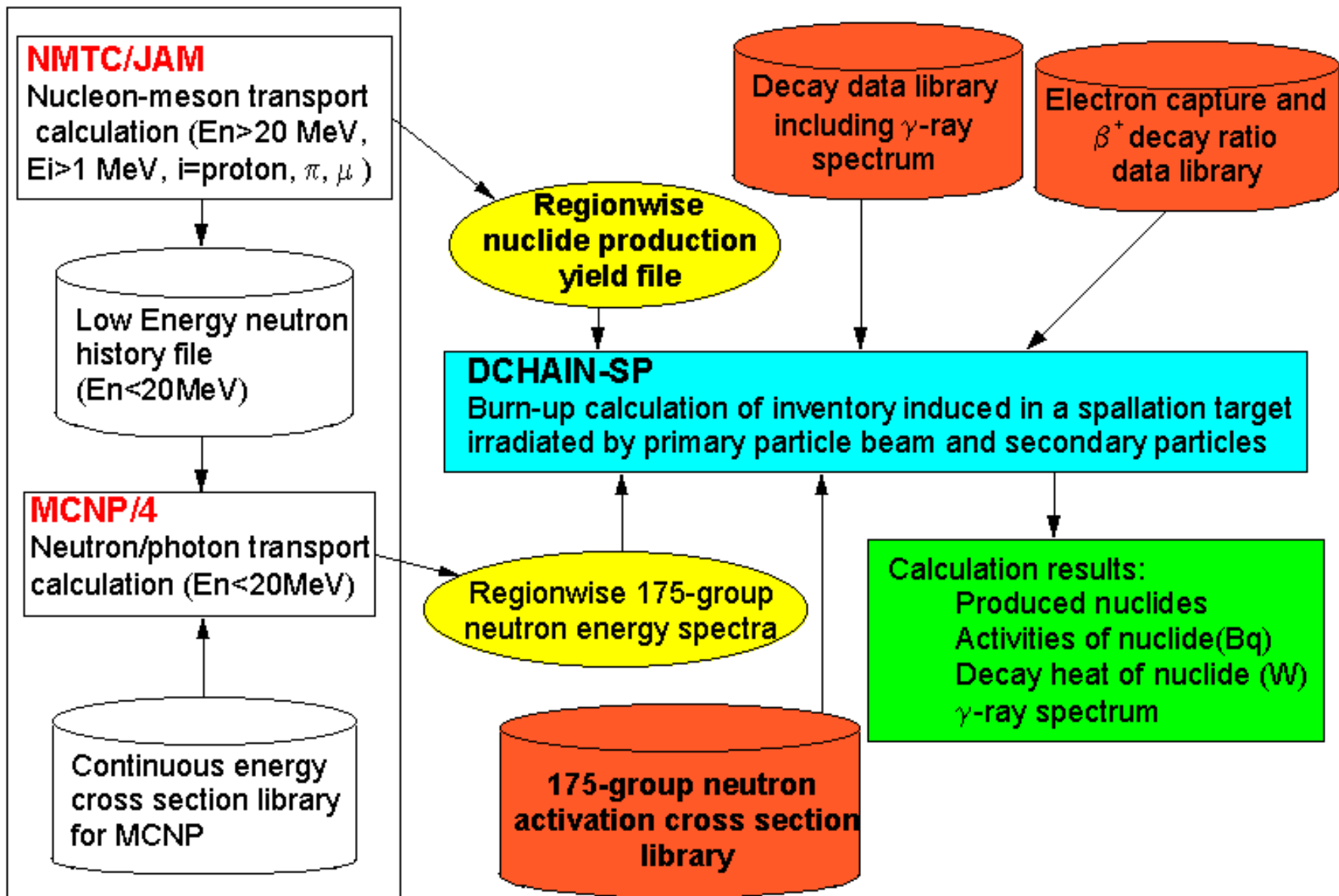


Validation of Radioactivity Calculation Code System

Tetsuya KAI, Fujio MAEKAWA, Yoshimi KASUGAI

Japan Atomic Energy Research Institute

Schematic diagram of DCHAIN-SP code system



Validation Process

1. Activation cross section library

(for neutrons below 20 MeV)

- Revision of FENDL/A-2.0
- Benchmarking by Experiments with 14-MeV neutron

2. Nuclide production yield

(for neutrons above 20 MeV, proton, pion, muon,...)

- Implementing GEM model in NMTC/JAM
- Adopting evaluated cross section data of He-4, N-14, O-16
- Comparison with experimental data

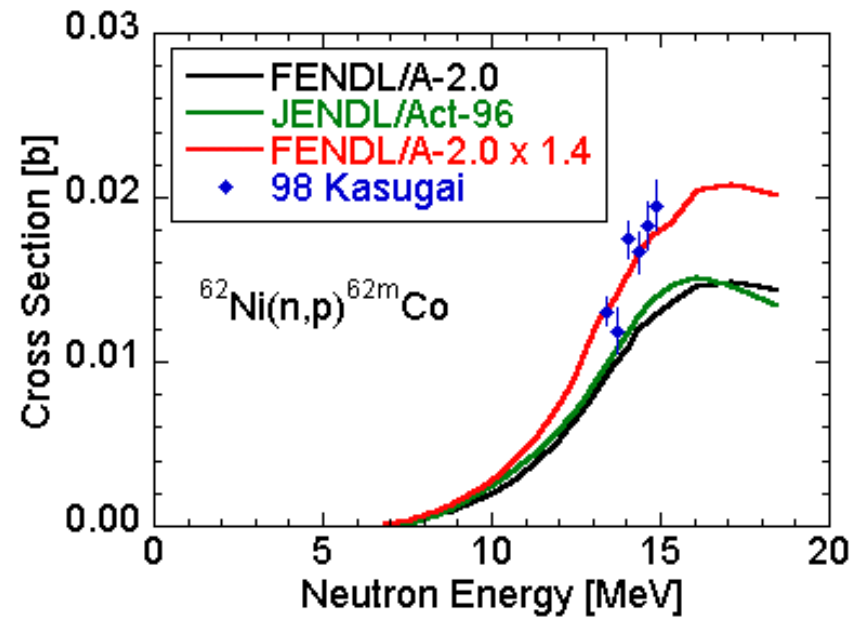
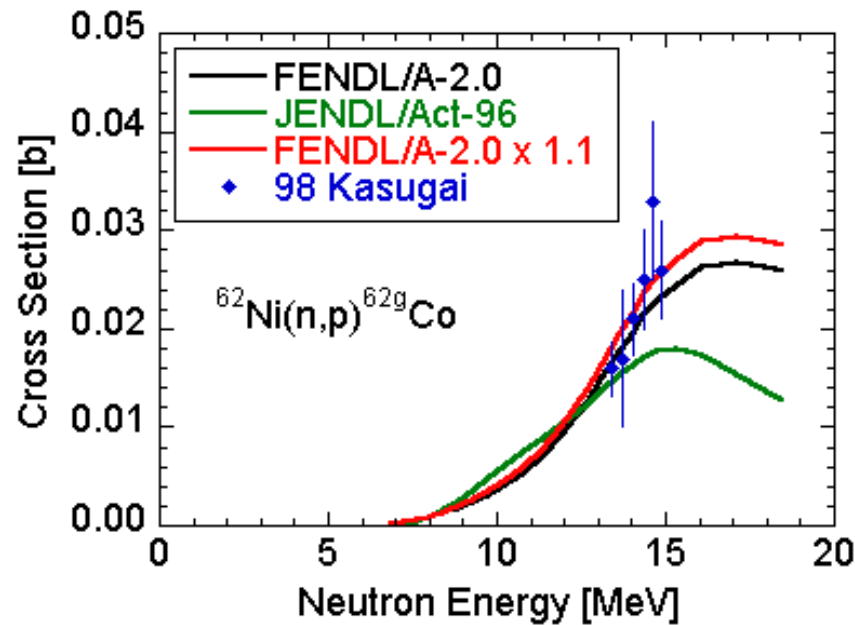
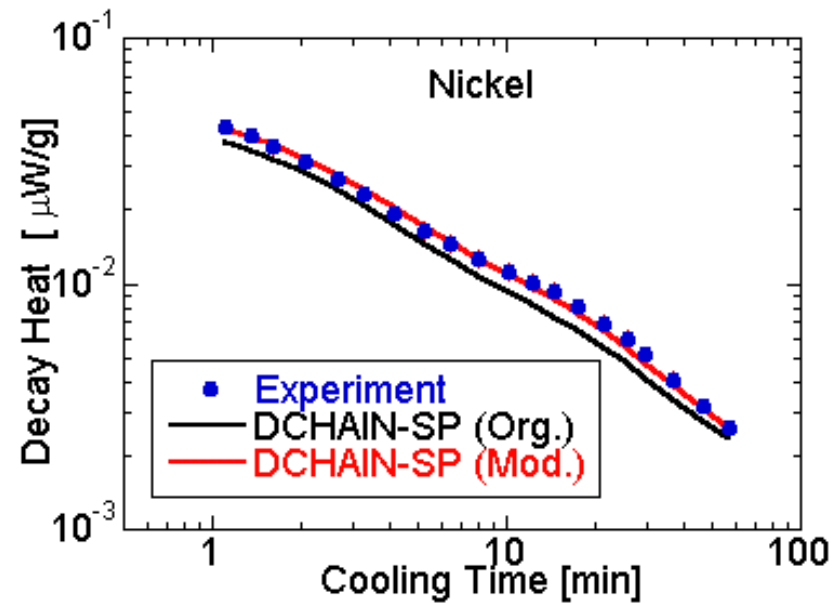
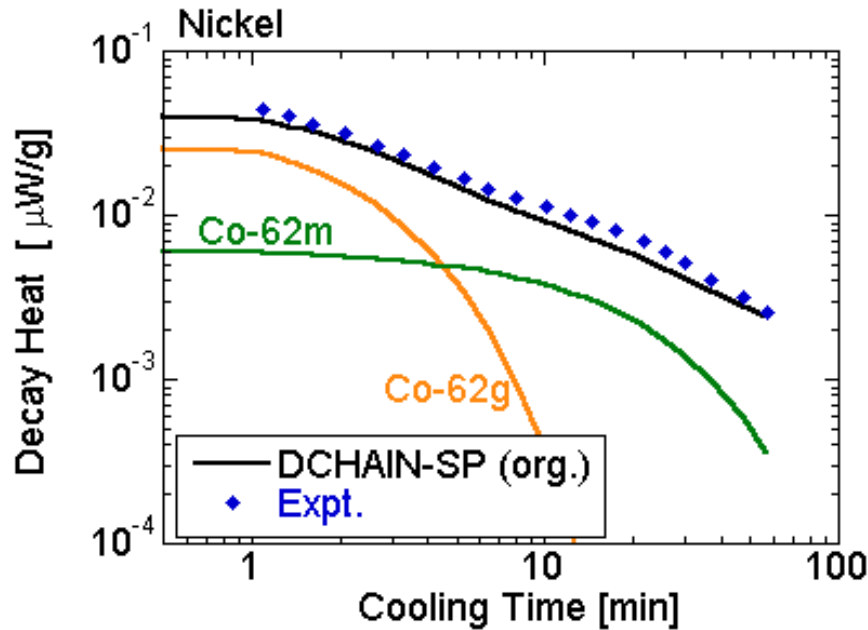
3. Whole code system

- Benchmarking by AGS activation experiment

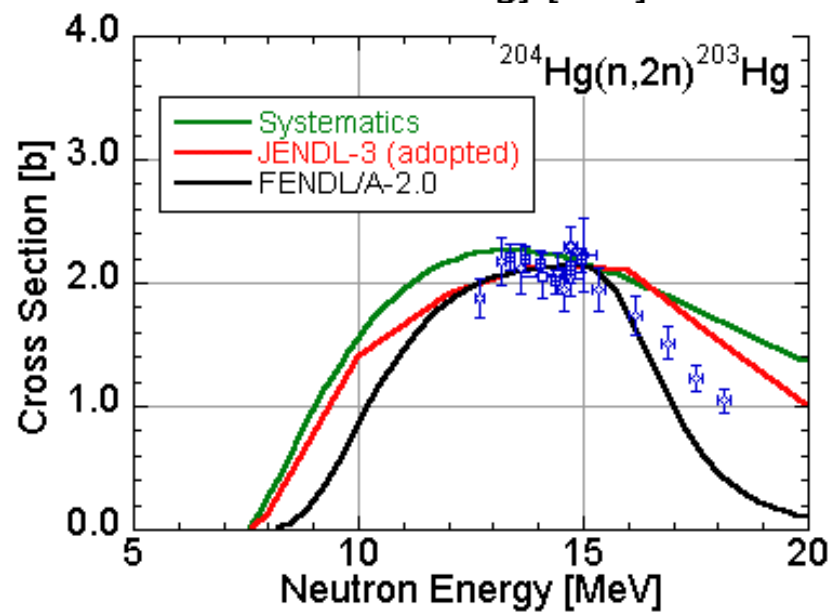
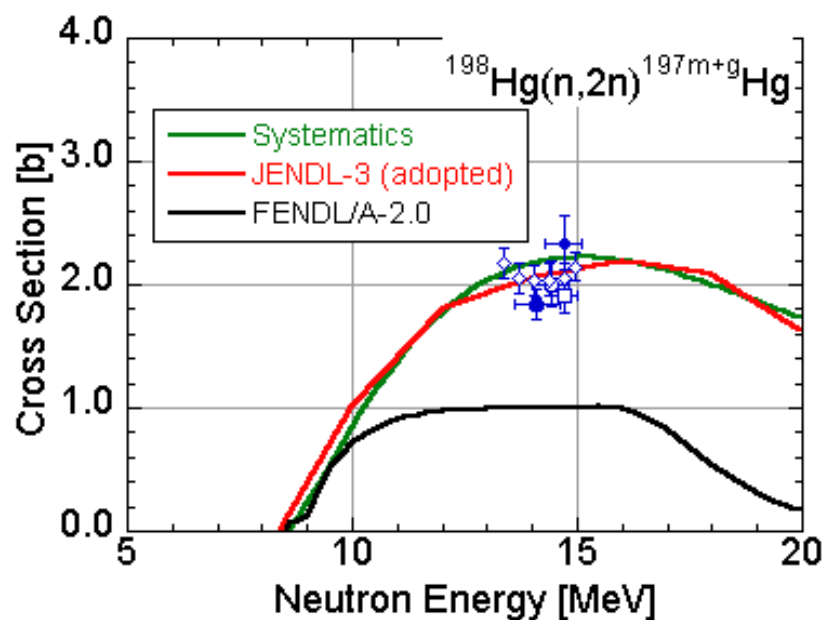
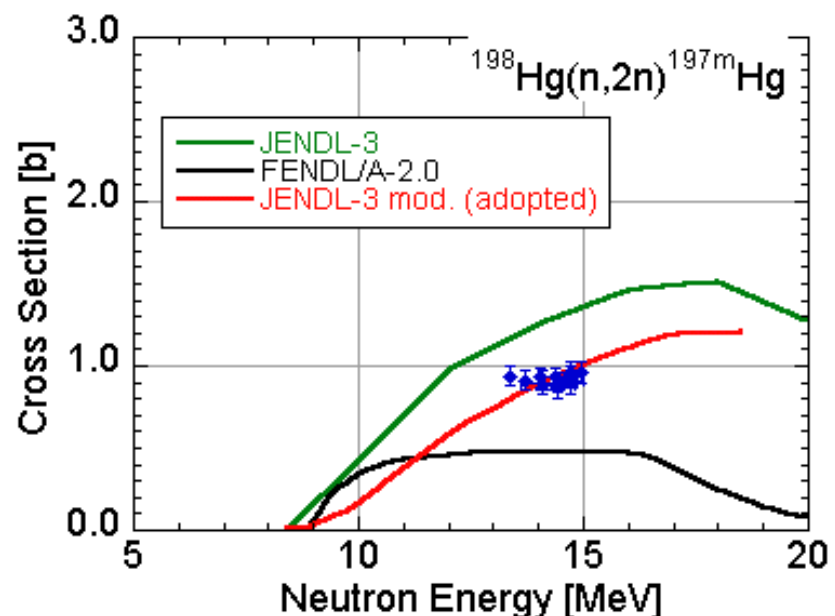
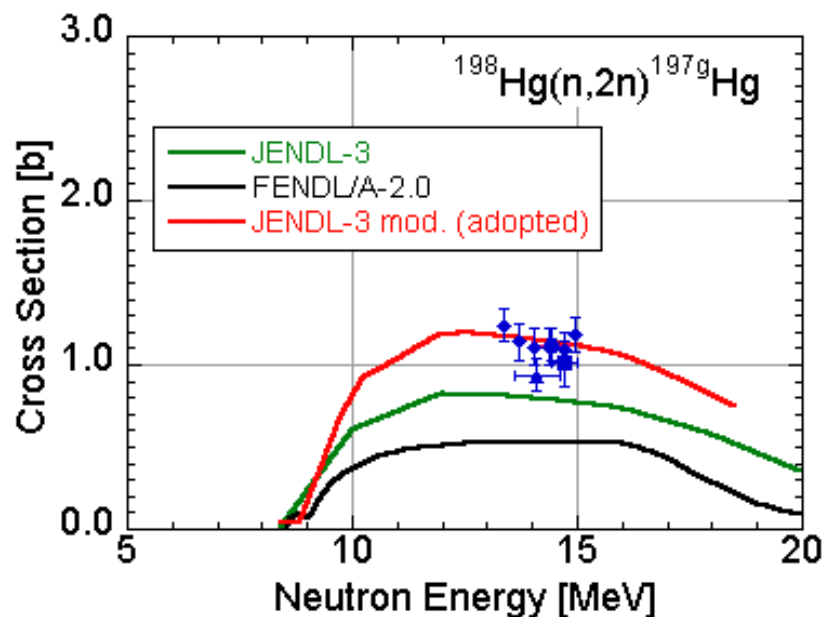
Revision of Cross Section Library FENDL/A-2.0

- Experiments by Fusion Neutronics Source
 - Decay heat of 32 fusion reactor materials
 - Activation cross section of Hg
 - Activity, decay heat of Hg
- Tritium production cross section
 - Existing experimental data, systematics

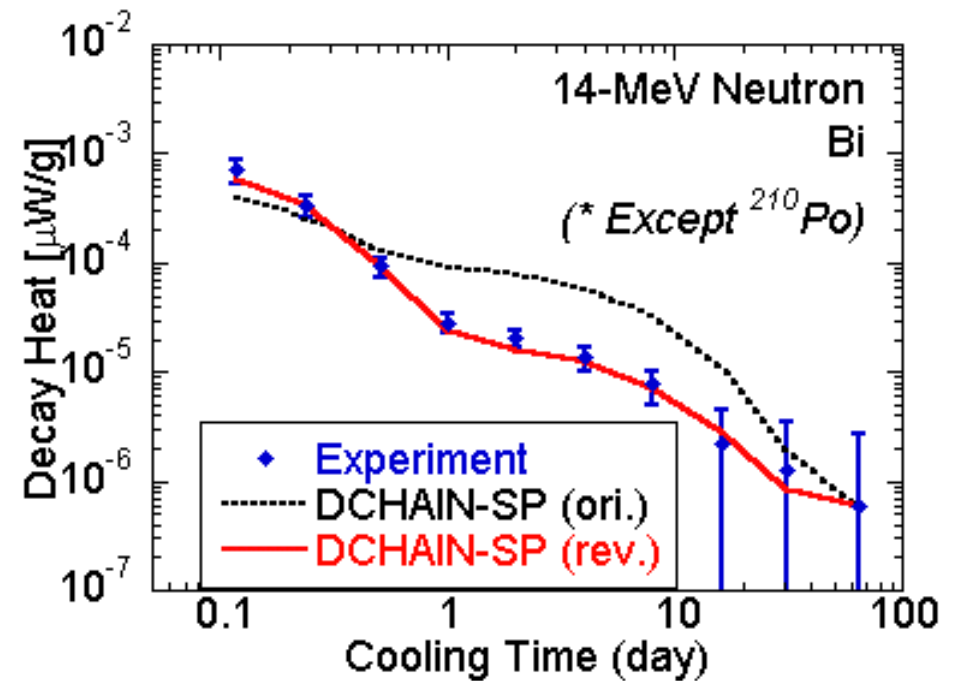
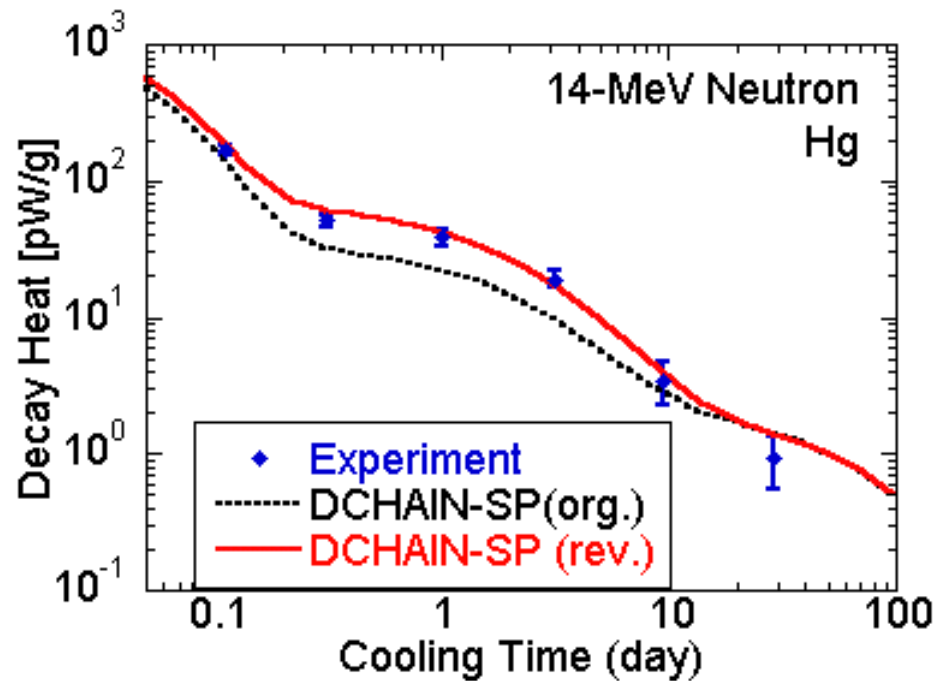
Revision of Cross Sections (Ni)



Revision of Cross Sections (Hg)



Improvements after Revision (Hg,Bi)



Lists of Revised Cross Section of FENDL/A-2.0 (1/2)

Revised Reaction	Data Source & Factor for Revision
$^{23}\text{Na}(n,2n)^{22}\text{Na}$	JENDL/Dosimetry-99
$^{23}\text{Na}(n,p)^{23}\text{Ne}$	JENDL/Act-96
$^{32}\text{S}(n,t)^{30}\text{P}$	JENDL/Act-96
$^{40}\text{Ca}(n,t)^{38}\text{K}$	FENDL/A-2.0 x 1/278.54
$^{50}\text{Ti}(n,p)^{50g}\text{Sc}, ^{50m}\text{Sc}$	JENDL/Act-96 x 1.1
$^{55}\text{Mn}(n,a)^{52}\text{V}$	FENDL/A-2.0 x 0.9
$^{55}\text{Mn}(n,p)^{55}\text{Cr}$	JENDL/Act-96
$^{58}\text{Ni}(n,p)^{58g}\text{Co}, ^{58m}\text{Co}$	JENDL/Act-96, low energy tail eliminated
$^{62}\text{Ni}(n,p)^{62g}\text{Co}$	FENDL/A-2.0 x 1.1
$^{62}\text{Ni}(n,p)^{62m}\text{Co}$	FENDL/A-2.0 x 1.4
$^{63}\text{Cu}(n,a)^{60g}\text{Co}, ^{60m}\text{Co}$	FENDL/A-2.0 x 1.2
$^{88}\text{Sr}(n,2n)^{87m}\text{Sr}$	FENDL/A-2.0 x 1.1
$^{88}\text{Sr}(n,p)^{88}\text{Rb}$	JENDL/Act-96 x 1.3
$^{89}\text{Y}(n,a)^{86m}\text{Rb}$	FENDL/A-2.0 x 2.0
$^{92}\text{Mo}(n,2n)^{91g}\text{Mo}, ^{91m}\text{Mo}$	JENDL/Act-96
$^{112}\text{Sn}(n,2n)^{111}\text{Sn}$	JENDL/Act-96 x 1.15
$^{118}\text{Sn}(n,p)^{118g}\text{In}, ^{118m1}\text{In}, ^{118m2}\text{In}$	FENDL/A-2.0 x 1.6
$^{120}\text{Sn}(n,p)^{120g}\text{In}, ^{120m1}\text{In}, ^{120m2}\text{In}$	FENDL/A-2.0 x 1.5
$^{185}\text{Re}(n,2n)^{184g}\text{Re}, ^{184m}\text{Re}$	FENDL/A-2.0 x 0.8
$^{181}\text{Ta}(n,2n)^{180g}\text{Ta}$	JENDL/Act-96
$^{184}\text{W}(n,p)^{184}\text{Ta}$	JENDL/Act-96
$^{186}\text{W}(n,2n)^{185g}\text{W}, ^{185m}\text{W}$	m/g ratio modified
$^{186}\text{W}(n,p)^{186}\text{Ta}$	FENDL/A-2.0 x 0.8

Revised Reaction	Data Source & Factor for Revision
$^{196}\text{Hg}(n,2n)^{196g}\text{Hg}$	JENDL-3.3 x 1.4
$^{196}\text{Hg}(n,2n)^{196m}\text{Hg}$	JENDL-3.3
$^{198}\text{Hg}(n,2n)^{197g}\text{Hg}, ^{197m}\text{Hg}$	JENDL-3.3, m/g ratio modified
$^{198}\text{Hg}(n,p)^{198g}\text{Au}$	FENDL/A-2.0 x 1.6
$^{199}\text{Hg}(n,2n)^{198}\text{Hg}$	JENDL-3.3
$^{199}\text{Hg}(n,n)^{199m}\text{Hg}$	FENDL/A-2.0 x 0.6
$^{199}\text{Hg}(n,p)^{199}\text{Au}$	FENDL/A-2.0 x 1.6
$^{200}\text{Hg}(n,2n)^{199g}\text{Hg}, ^{199m}\text{Hg}$	JENDL-3.3
$^{200}\text{Hg}(n,p)^{200m}\text{Au}$	FENDL/A-2.0 x 5.0
$^{201}\text{Hg}(n,2n)^{200}\text{Hg}$	JENDL-3.3
$^{201}\text{Hg}(n,p)^{201}\text{Au}$	FENDL/A-2.0 x 2.0
$^{202}\text{Hg}(n,2n)^{201}\text{Hg}$	JENDL-3.3
$^{202}\text{Hg}(n,p)^{202}\text{Au}$	JENDL-3.3
$^{204}\text{Hg}(n,2n)^{203}\text{Hg}$	JENDL-3.3
$^{204}\text{Hg}(n,p)^{204}\text{Au}$	JENDL-3.3
$^{204}\text{Pb}(n,2n)^{203g}\text{Pb}, ^{203m}\text{Pb}$	JENDL-3.2, m/g ratio from FENDL/A-2.0
$^{208}\text{Pb}(n,p)^{208}\text{Tl}$	FENDL/A-2.0 x 1.5
$^{209}\text{Bi}(n,p)^{209}\text{Pb}$	FENDL/A-2.0 x 2.0
$^{209}\text{Bi}(n,g)^{210g}\text{Bi}, ^{210m}\text{Bi}$	JENDL/Act-96

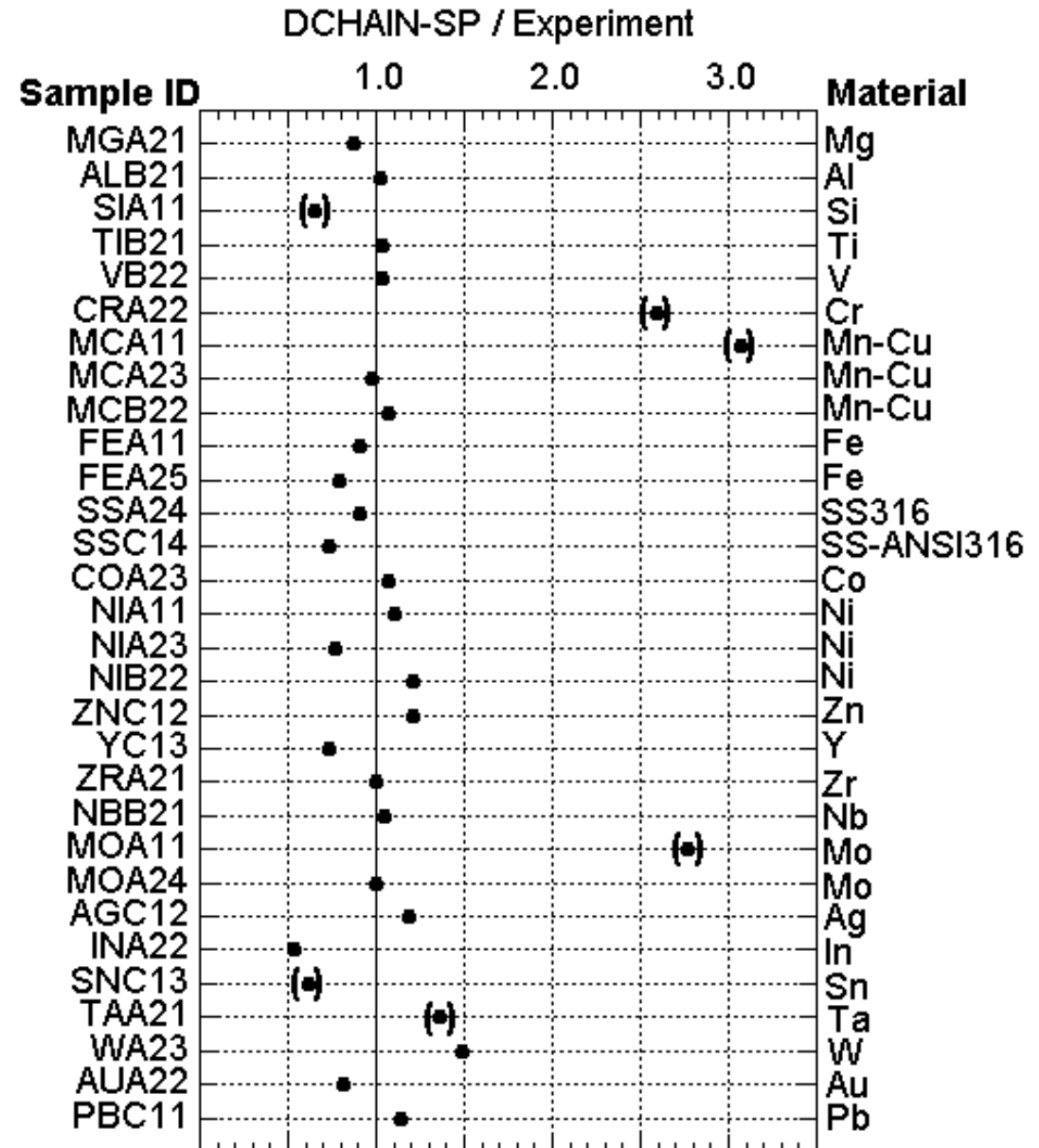
Lists of Revised Cross Section of FENDL/A-2.0 (2/2)

Revised Reaction	Data Source & Factor for revision
$^{10}\text{B}(n,t)^8\text{Be}$	FENDL/A-2.0 x 1.5
$^{16}\text{O}(n,t)^{14}\text{N}$	FENDL/A-2.0 x 0.02
$^{17}\text{O}(n,t)^{15}\text{N}$	FENDL/A-2.0 x 10
$^{18}\text{O}(n,t)^{16}\text{N}$	FENDL/A-2.0 x 100
$^{19}\text{F}(n,n't)^{16}\text{O}$	FENDL/A-2.0 x 0.1
$^{46}\text{Ti}(n,t)^{44m}\text{Sc}, ^{44g}\text{Sc}$	FENDL/A-2.0 x 0.2
$^{51}\text{V}(n,t)^{49}\text{Ti}$	FENDL/A-2.0 x 10
$^{53}\text{Cr}(n,t)^{51}\text{V}$	FENDL/A-2.0 x 0.1
$^{54}\text{Cr}(n,t)^{52}\text{V}$	FENDL/A-2.0 x 0.1
$^{54}\text{Fe}(n,t)^{52m}\text{Mn}$	FENDL/A-2.0 x 0.01
$^{54}\text{Fe}(n,t)^{52g}\text{Mn}$	FENDL/A-2.0 x 0.1
$^{57}\text{Fe}(n,t)^{55}\text{Mn}$	FENDL/A-2.0 x 5
$^{58}\text{Fe}(n,t)^{56}\text{Mn}$	FENDL/A-2.0 x 5
$^{65}\text{Cu}(n,t)^{63}\text{Ni}$	FENDL/A-2.0 x 10
$^{83}\text{Kr}(n,t)^{81}\text{Br}$	FENDL/A-2.0 x 0.1
$^{92}\text{Mo}(n,t)^{90m}\text{Nb}, ^{90g}\text{Nb}$	FENDL/A-2.0 x 0.01
$^{151}\text{Eu}(n,t)^{149}\text{Sm}$	FENDL/A-2.0 x 0.1
$^{152}\text{Eu}(n,t)^{150}\text{Sm}$	FENDL/A-2.0 x 0.1
$^{153}\text{Eu}(n,t)^{151}\text{Sm}$	FENDL/A-2.0 x 0.1
$^{154}\text{Eu}(n,t)^{152}\text{Sm}$	FENDL/A-2.0 x 0.1
$^{197}\text{Au}(n,t)^{195}\text{Pt}$	FENDL/A-2.0 x 0.2
$^{239}\text{Pu}(n,t)^{237}\text{Np}$	FENDL/A-2.0 x 200

Calculation Test on γ -ray Energy Release

- Total energy release of secondary γ -ray
- DCHAIN-SP can predict most of experimental data within several tens of percent.

* Large discrepancies indicated in parenthesis are not due to the DCHAIN-SP calculations.



Implementing GEM model in NMTC/JAM

- GEM model is implemented in NMTC/JAM to obtain accurate prediction of the cross section of light fragments such as beryllium produced from proton-induced reactions.

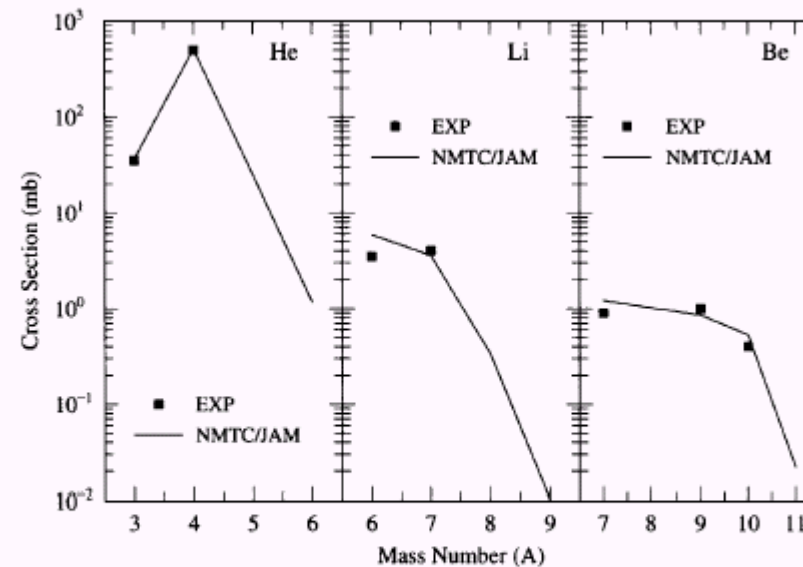


Figure 15. The isotope production cross sections of He, Li and Be from the Ag(p,x) reaction at 480 MeV. The experimental data are taken from Ref. ⁴²⁾. The results of JAM with GEM are shown by the solid lines.

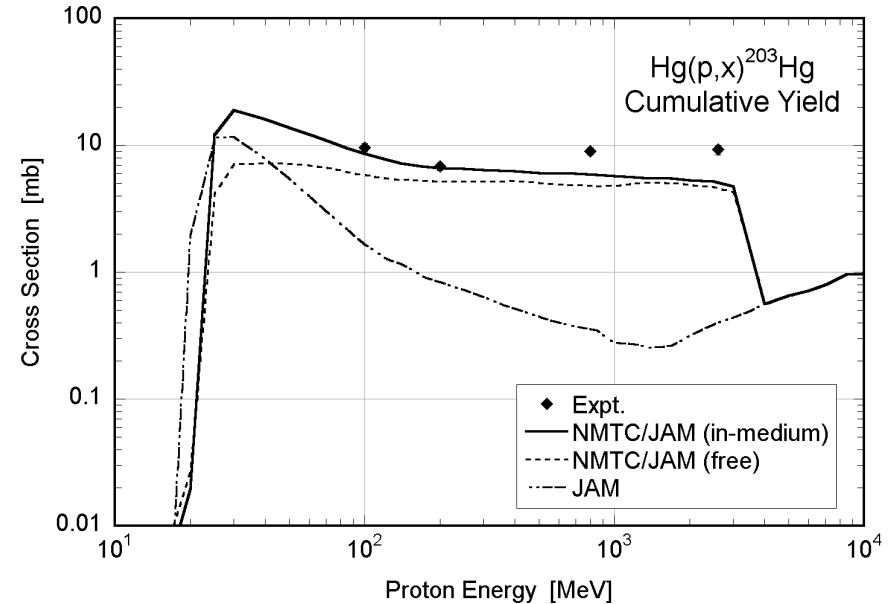
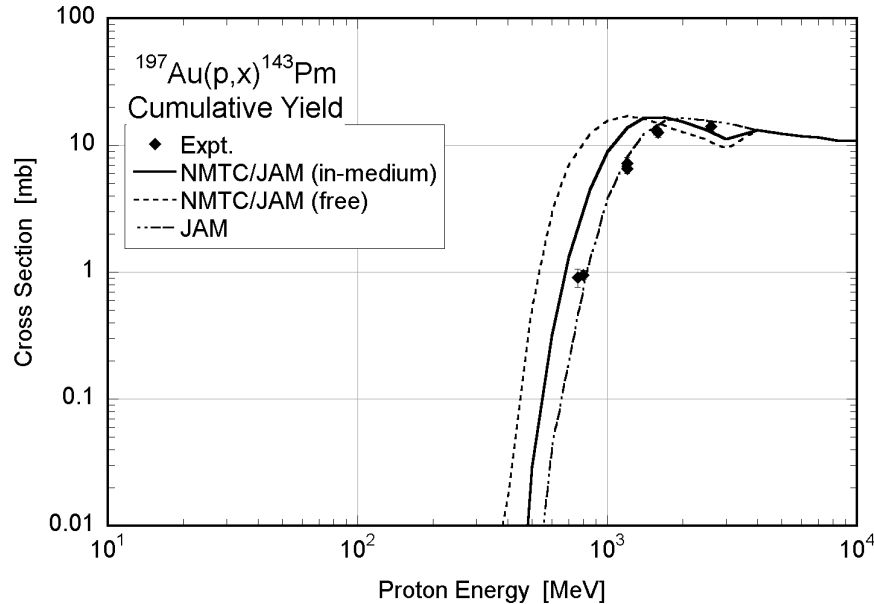
Adopting Evaluated Cross Section Data of He-4, N-14, O-16

- NMTC/JAM adopted a function to calculate the production rates from helium-4, nitrogen-14 and oxygen-16 using cross section data sets made from experimental data automatically.

${}^4\text{He}(n,x){}^3\text{H}$	${}^{14}\text{N}(n,x){}^3\text{H}$	${}^{14}\text{N}(n,x){}^7\text{Be}$	${}^{14}\text{N}(n,x){}^{11}\text{Be}$	${}^{14}\text{N}(n,x){}^{10}\text{C}$	${}^{14}\text{N}(n,x){}^{11}\text{C}$
${}^{14}\text{N}(n,x){}^{14}\text{C}$	${}^{14}\text{N}(n,x){}^{13}\text{N}$	${}^{16}\text{O}(n,x){}^3\text{H}$	${}^{16}\text{O}(n,x){}^7\text{Be}$	${}^{16}\text{O}(n,x){}^{11}\text{Be}$	${}^{16}\text{O}(n,x){}^{10}\text{C}$
${}^{16}\text{O}(n,x){}^{11}\text{C}$	${}^{16}\text{O}(n,x){}^{14}\text{C}$	${}^{16}\text{O}(n,x){}^{15}\text{C}$	${}^{16}\text{O}(n,x){}^{13}\text{N}$	${}^{16}\text{O}(n,x){}^{16}\text{N}$	${}^{16}\text{O}(n,x){}^{14}\text{O}$
${}^{16}\text{O}(n,x){}^{15}\text{O}$	${}^4\text{He}(p,x){}^3\text{H}$	${}^{14}\text{N}(p,x){}^7\text{Be}$	${}^{14}\text{N}(p,x){}^{11}\text{Be}$	${}^{14}\text{N}(p,x){}^{10}\text{C}$	${}^{14}\text{N}(p,x){}^{11}\text{C}$
${}^{14}\text{N}(p,x){}^{13}\text{N}$	${}^{14}\text{N}(p,x){}^{14}\text{O}$	${}^{16}\text{O}(p,x){}^3\text{H}$	${}^{16}\text{O}(p,x){}^7\text{Be}$	${}^{16}\text{O}(p,x){}^{11}\text{Be}$	${}^{16}\text{O}(p,x){}^{10}\text{C}$
${}^{16}\text{O}(p,x){}^{11}\text{C}$	${}^{16}\text{O}(p,x){}^{14}\text{C}$	${}^{16}\text{O}(p,x){}^{13}\text{N}$	${}^{16}\text{O}(p,x){}^{14}\text{O}$	${}^{16}\text{O}(p,x){}^{15}\text{O}$	

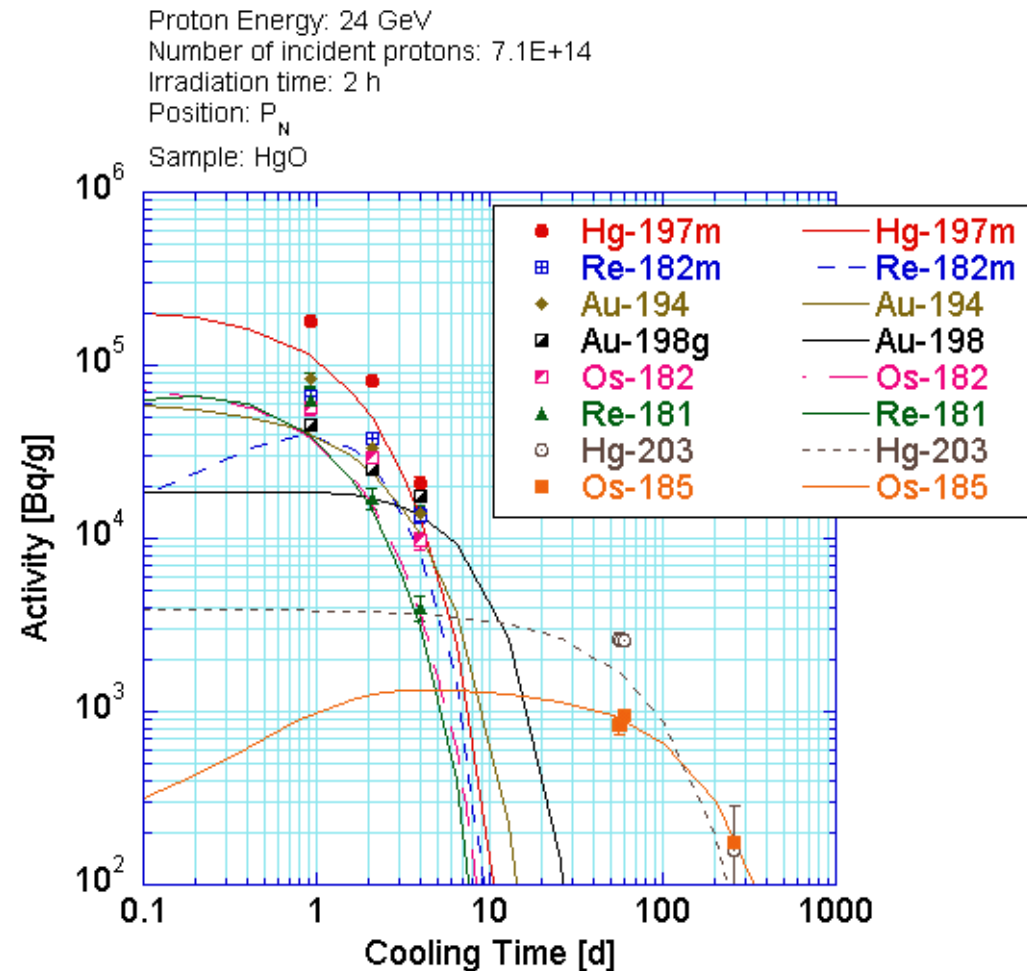
Comparison with experimental data & NMTC/JAM

- Proton-induced nuclide production yield.
- Target: C, N, O, Al, Ca, Fe, Cu, Nb, Ba, Au, Hg, Pb, Bi, U
- Proton energy: 10MeV ~ 10 GeV
- 685 reactions
- Experimental data were mainly cited from EXFOR.



Benchmarking by AGS activation experiment

- An activation experiment on carbon, oxygen, boron-10, boron-11, aluminum, copper, iron, niobium, lead, bismuth and mercury using 3 and 24 GeV proton at AGS/BNL was carried out.



Summary

- DCHAIN-SP Code system can predict radioactivity with adequate accuracy.